Identification of Hydrodynamic Derivatives for Ship Maneuvering Prediction in Restricted Waters

Conference Paper · September 2013

CITATIONS
4

READS
540

2 authors:

Philipp Mucha
Siemens USA
16 PUBLICATIONS **60** CITATIONS
SEE PROFILE

Ould el Moctar
University of Duisburg-Essen
136 PUBLICATIONS **749** CITATIONS
SEE PROFILE

Identification of Hydrodynamic Derivatives for Ship Maneuvering Prediction in Restricted Waters

Philipp Mucha and Bettar el Moctar*

1 INTRODUCTION

This paper investigates the identification of hydrodynamic derivatives for ships sailing in restricted waters and discusses their influence on course keeping stability. Planar Motion Mechanism (PMM) tests are numerically replicated drawing upon the solution of the Reynolds-averaged Navier-Stokes (RANS) equations. Both lateral and vertical flow restrictions are considered in systematic pure sway and yaw tests. The powerful influence canal walls or river topologies exert upon ships is notorious among pilots and hydrodynamicists because these effects aggrevate both ship handling and maneuvering prediction. While new vessels in inland waterway shipping tend to grow in size, existing waterways do not - this in turn imposes increased challenges to ensure safe and easy traffic. In this context maneuvering prediction methods become more important.

Related Work. Abundant discussions of ship hydrodynamics in restricted waters and numerical methods for prediction can be found in Tuck (1978), Newman (1978) and reference therein. More recently, investigations covering both Boundary Element Methods (BEM) and RANS-CFD relate to the International Conference on Ship Maneuvering in Shallow and Confined Waters (*e.g.* Liu, 2011) or the SIMMAN workshop (Stern et al., 2008). For the present study, the work of Thomas and Sclavounos (2006) is of special interest since it expands on the subject of hydrodynamic interaction forces in light of their influence on dynamic stability.

Organization of the Paper. The addressed maneuvering theory, the PMM test method and the numerical technique to model the ship flow is introduced first. Then, the virtual PMM test method is applied to derive sway and yaw acceleration derivatives for a spheroid. These are compared to related theoretical values from the literature. Specific light is shed on the test parameters and the numerical technique involved. Drawing upon these results for unrestricted flow the influence of a vertical wall and underkeel clearance is investigated. Finally the method is applied to a typical vessel encountered on German inland waterways. The resulting set of hydrodynamic derivatives populates a simple linear maneuvering model for various restricted maneuvering environments. The influence on course keeping stability is addressed stemming from the analysis of the dynamic systems' eigenvalues.

*Philipp Mucha is with the Institute of Ship Technology, Ocean Engineering and Transport Systems (ISMT, University of Duisburg-Essen) and the German Federal Waterways Engineering and Reserach Institute (BAW). Bettar el Moctar is with ISMT. Email: philipp.mucha@uni-due.de, ould.el-moctar@uni-due.de

2 MANEUVERING THEORY

Newtonian mechanics are applied to a ship under rigid body and constant mass assumption leading to the maneuvering equations of motion. Their formulation is given for a ship-fixed Cartesian coordinate system x, y, z the origin of which coincides with the ship's longitudinal and transverse midpoint dimensions. x is pointing forward, y to starboard and z downward. The ship trajectory is given for an earth-fixed reference system x_0, y_0, z_0. For maneuvering purposes the equations of motion in six degrees of freedom are reduced to describe only those motions in the horizontal plane:

$$m\left(\dot{u} - vr - x_g r^2\right) = X \tag{1}$$

$$m\left(\dot{v} + ur + x_g \dot{r}\right) = Y \tag{2}$$

$$I_z \dot{r} + m x_g \left(\dot{v} + ur\right) = N \tag{3}$$

In (1-3) m is the ship mass and I_z the moment of inertia about the vertical axis. The rigid body velocities in surge, sway and yaw are denoted by u, v and r, respectively. The center of gravity takes coordinates x_g, y_g, z_g. Temporal derivatives are denoted with a dot. X is the external force in longitudinal direction, Y in transverse direction and N the external moment about the ship's vertical axis, respectively. A customary and straightforward approach to express the external forces is their formulation in terms of a Taylor-series expansion about an equilibrium state. If only small deviations from this state are considered a linear framework will suffice to cast the system dynamics. Moreover, for constant forward speed the surge mode can be excluded. The quantities arising from the Taylor-series expansion and acting on the state variables are known as the hydrodynamic derivatives. The maneuvering equations can be rearranged to constitute a classic linear mass-damper system:

$$\begin{bmatrix} -Y_{\dot{v}} + m & -Y_{\dot{r}} + m x_g \\ -N_{\dot{v}} + \Delta x_g & -N_{\dot{r}} + I_z \end{bmatrix} \begin{bmatrix} \dot{v} \\ \dot{r} \end{bmatrix} + \begin{bmatrix} -Y_v & -Y_r + (m - X_{\dot{u}})U_1 \\ -N_v + (X_{\dot{u}} - Y_{\dot{v}})U_1 & -N_r + (m - Y_{\dot{r}})U_1 \end{bmatrix} \begin{bmatrix} v \\ r \end{bmatrix} = \begin{bmatrix} -Y_{\delta_R} \\ -N_{\delta_R} \end{bmatrix} \begin{bmatrix} \delta_R \end{bmatrix} \tag{4}$$

Table 1: MOTION PARAMETERS FOR PMM TESTS WITHIN AN EARTH-FIXED FRAME

Motion	Pure sway	Pure yaw
u	u_0	u_0
v	$-y_{max}\omega cos(\omega t)$	$-y_{max}\omega cos(\omega t)$
r	0	$\psi_{max}\omega sin(\omega t)$

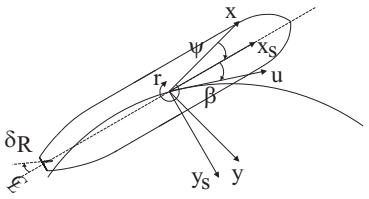

Figure 1: COORDINATE SYSTEMS FOR SHIP MANEUVERING

The subscripts in X, Y and N denote the quantities with respect to which the partial derivatives are taken. For ship-like bodies the hydrodynamic derivative $X_{\dot{u}}$ is considerably lower than the ship's mass and can be dropped from the equations. A way to identify these coefficients is the PMM method. Through dynamic tests in which a harmonic motion is superponed to a forward motion at constant speed, both acceleration and velocity derivatives can be found. The periodic time series of the measured or computed forces are then referred to the Taylor series and subjected to Fourier analysis. Within the linear framework the expression for Y in pure sway mode then reads

$$Y = Y_{\dot{v}}\dot{v} + Y_v v \tag{5}$$

In line with the motion formulation within an earth-fixed coordinate system provided by Table 1 its harmonic representation is

$$Y(t) = Y_{S1}sin(\omega t) + Y_{C1}cos(\omega t) \tag{6}$$

and the derivatives of interest are finally found from

$$Y_{\dot{v}} = \frac{Y_{S1}}{v_A\omega} \tag{7}$$

$$Y_v = -\frac{Y_{C1}}{v_A} \tag{8}$$

v_A is the sway velocity amplitude as per $y_{max}\omega$ where y_{max} is the lateral displacement and ω the frequency of the harmonic motion. The test parameters are chosen in accordance with the guidelines and recommendations of the ITTC (2005). For pure sway a nondimensional frequency $\omega'=\omega L/u_0$ of typically 1-2 and of 2-4 for pure yaw tests is suggested. L is the ship length. An extensive coverage of this procedure can be found in Yoon (2009). The linear assumption behind (5-8) is noteworthy: the force is assumed to be exclusively dependent on the contemporary velocity and acceleration, thus unaffected by memory effects.

3 NUMERICAL METHOD

A dynamic equation describing the motion of a viscous and incompressible flow is found from turning to the Navier-Stokes equations. The integral representation of the mass and momentum conservation equations satisfies

$$\frac{\partial}{\partial t}\int_V \rho \,\mathrm{d}V + \int_S \rho \mathbf{v}\cdot\mathbf{n}\,\mathrm{d}S = 0 \tag{9}$$

$$\frac{\partial}{\partial t}\int_V \rho\mathbf{v}\,\mathrm{d}V + \int_S \rho(\mathbf{vv})\cdot\mathbf{n}\,\mathrm{d}S = \int_S \mathbf{T}\cdot\mathbf{n}dS + \int_V \rho\mathbf{b}\,\mathrm{d}V \tag{10}$$

where $\mathbf{v}$ denotes the velocity vector, $\mathbf{n}$ is the normal vector of S which represents the area of the surface of the control volume V, $\mathbf{T}$ denotes the stress tensor and $\mathbf{b}$ a vector describing a force per unit mass.

The additional transport of momentum due to the turbulent nature of the flow is accounted for by expressing the flow quantities in terms of their time average and fluctuating parts leading to the RANS equations. A SST k-ω model (Menter, 1994), involving two more transport equations provides closure of the system of equations.

The flow equations are approximated by the Finite Volume (FV) method. The approximation of the flow equations for the entirety of control volumes (CVs) provides a set of algebraic equations. The flow equations are solved in a segregated fashion based on the Semi-Implicit Method for Pressure-Linked Equations (SIMPLE) algorithm. For an elaborate discussion the reader is referred to Ferziger and Peric (1996). An implicit temporal scheme of second order and three time levels is used for unsteady simulations. The present problem of conducting virtual PMM tests involves relative motions between the vessel and the spatial restrictions which calls for the modeling of transient mesh deformations (mesh morphing). The method redistributes mesh vertices following prescribed displacements of control points which are related to existing mesh vertices of the boundaries of the solution domain. The commercial solver STARCCM+ is used in the present investigation and a detailed formulation of the numerical method is given in Cd adapco (2013).

An inlet boundary condition is set one ship length upstream specifying the flow velocity and turbulent kinetic energy and disspiation rate. Two ship lengths downstream and one ship length away from the ship on the domain sides an outlet boundary condition holds where the pressure is given directly and velocities are found from the arithmetic average of neighboring cells. Inflow can be considered in terms of the normal component of boundary recirculation. If a lateral restriction

Table 2: MAIN PARTICULARS

	Length	Beam	Draft	c_B
Spheroid	2a=100m	2b=15m	7.5m	0.52
Vessel	110m	11.4m	3m	0.89

Table 3: GRID SENSITIVITY STUDY

CVs	$\frac{Y_{\dot{v}}}{\rho\nabla}$	$\frac{Y_v B}{\rho\nabla U}$	$\frac{N_{\dot{r}}}{0.2\rho\nabla(a^2+b^2)}$	$\frac{N_r B}{\rho\nabla UL}$
201894	-0.9538	-0.0382	-0.7472	-0.4228
252714	-0.9394	-0.0409	-0.7505	-0.4085
416824	-0.9422	-0.0408	-0.7560	-0.4079
Panels	$\frac{a_{22}}{\rho\nabla}$		$\frac{a_{66}}{0.2\rho\nabla(a^2+b^2)}$	
924	-0.9431		-0.7828	
1476	-0.9519		-0.7949	
3064	-0.9629		-0.8051	
Theory	-0.9600		-0.8000	

is considered the domain boundary on the starboard side of the vessel at distance *d* turns into a free slip wall (zero normal velocity component). The bottom and top boundaries are also given free slip wall conditions. If free surface flow is to be modeled the Volume of Fluid (VOF) technique is used (Ferziger and Peric, 1996). The ship boundary is a no-slip wall (zero tangential velocity component). For rigid body motions the ship boundary vertices are assigned respective velocities and the rigid free surface is allowed to experience in-plane deformations.

4 RESULTS AND DISCUSSION

The Spheroid. In lack of experimental data for validation purposes comparison can be drawn to results found from analytic scrutiny. Such information exists for added masses of simple bodies based upon potential flow theory (Newman, 1978). In three dimensions such a simple body is a spheroid the sway added mass a_{22} and yaw added moment of inertia a_{66} of which are quantified in the reference. The flow is assumed unbounded, it does not consider the influence of waves. The hydrodynamic forces arising from the body acceleration in sway and yaw mode of motion will be proportional to just the above quantities, it might be compared to the respective acceleration derivatives as present in (4). The comparison can serve as a check for the suitability of the numerical method albeit their identification is done within a viscous flow regime. The main particulars of the spheroid are given in Table 2.

Preliminaries. A forward speed of 3m/s corresponding to Reynolds-Number Re=3·10^9 is used. Due to the low Froude Number (F_n=0.095) the free surface is considered rigid leading to the classical double-body flow. It is obvious from (5-8) that the hydrodynamic derivatives are functions of both test frequency and amplitude. In favor of reduced testing effort in the single-run PMM method only one test is conducted at low frequency, assumed to be sufficiently close to zero to obtain the slow motion derivatives. The periodic time series of the side force and yaw moment are smoothed by the moving average method before they are subjected to Fourier analysis. The oscillation is observed to be stable after one quarter of an oscillation and shows convergent behavior (constant amplitude oscillation) after three oscillations. Computations are performed on a High Performance Computer (HPC) cluster on four Intel(R) Sandy Bridge nodes (64 cores).

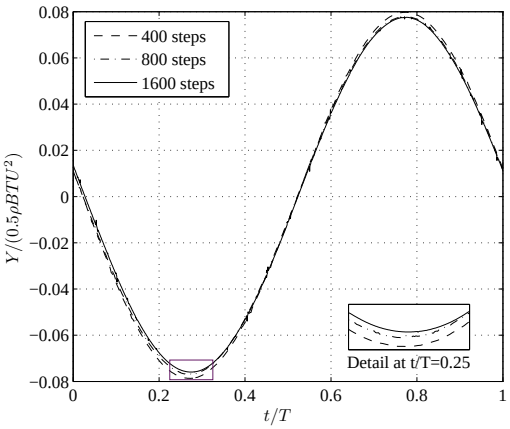

Figure 2: TIME STEP SENSITIVITY STUDY: NONDIMENSIONAL SIDE FORCE AGAINST THE RATIO OF TIME t TO OSCILLATION PERIOD T

Sensitivity Studies. PMM tests are performed using three grids with a refinement factor of $\sqrt{2}$. The near wall discretization is chosen in accordance with the wall function used. It remains constant during the refinement. The test parameters are ω'=2 and y_A=1m for pure sway and ω'=4 and ψ_A=2.3° for pure yaw. Comparison is also drawn to a_{22} and a_{66} computed with the zero-speed Green Function method of the code GLRankine (Söding, 2012). Table 3 shows that the difference in $Y_{\dot{v}}$ between the grids is less than 2%. The result from the finest grid differs by 1.88% from the theoretical sway added mass. The sway velocity derivative Y_v deviates by 6.6% between the coarse and the fine grid —here there is no theoretical value available. For $N_{\dot{r}}$ the maximum deviation between the grids is less than 2% and for N_r its 3.5%. $N_{\dot{r}}$ computed with the finest grid is 5.5% less than the theoretical value. It has to be kept in mind that the frequency dependence is not considered yet. The zero speed Green Function method approaches the theoretical values with increasing body panels for both quantities. On the medium size FV grid the computational time for one period of oscillation T=104.72s with 800 time steps is approximately seven minutes. The

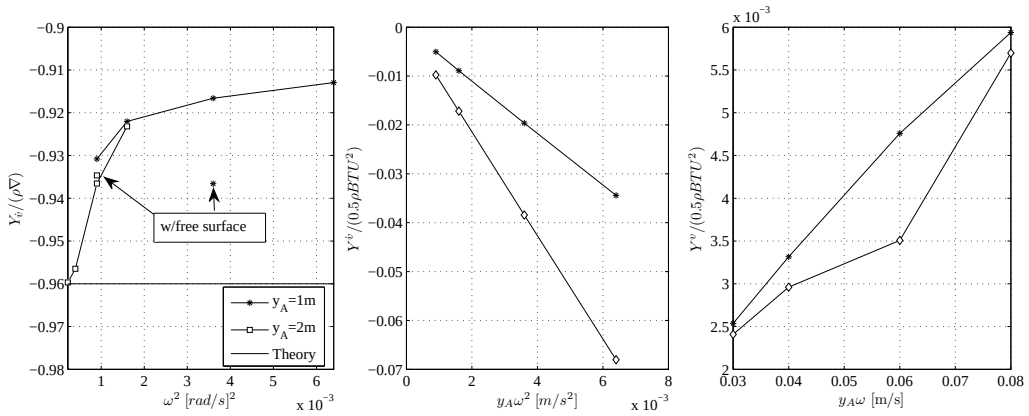

Figure 3: PARAMETER STUDY FOR SWAY FORCE DERIVATIVES

grid with free surface considered comprised $1{\cdot}10^6$ cells and for the case ω'=2 the computational time is about 30 minutes per oscillation. The added masses found from GLR are readily available within less than a minute on a common desktop computer. The sensitivity to temporal discretization is checked by varying the time step to yield 400, 800 and 1600 steps per oscillation. Figure 2 illustrates the result of this study for a pure sway test. The trends for the two finer time steps do not show a marked difference in Y. 800 steps per oscillation and the medium size grid are chosen throughout forthcoming simulations.

Figure 3 illustrates the test paramter study for lateral force components found from pure sway tests. The left hand side plot shows $Y_{\dot{v}}$ as a function of ω^2 and for two amplitudes y_A. $Y_{\dot{v}}$ takes higher norm values the smaller the frequency gets, this trend approaches the theoretical value. The lowest frequency corresponds to the smallest ITTC reccomendation ω'=0.25 and the highest frequency is equivalent to ω'=4. Results scatter around the reference value by maximum 5%. For two cases the free surface has been taken into account and results differ by less than 3% compared to the double-body flow. The right hand side plots show the force contributions without normalization to derivative representation as a function of sway velocity $y_A\omega$ and acceleration $y_A\omega^2$ for the amplitudes considered. By varying the flow history memory effects and nonlinearities involved in the testing procedure can be identified (Renilson, 1986). The difference between the amplitude curves indicates memory effects. The deviation of these curves from a straight line reveals nonlinearities. The linear assumption appears to be well suited for $Y^{\dot{v}}$ and memory effects become pronounced for higher frequencies. For Y^{v} no such straight line is observed and more tests would be necessary to gain insight into the dependencies. Throughout forthcoming simulations pure sway tests are performed with ω'=1 and y_A=2m. For pure yaw tests, ω'=4 and ψ_A=2.3° are used. In general amplitudes are kept low in light of the runs in laterally restricted flow.

Restricted Flow. Figure 5 depicts the linear sway force derivatives as a function of the nondimensional distance to the wall d/L. Both $Y_{\dot{v}}$ and Y_v increase in a nonlinear fashion. This trend agrees with investigations carried out for a slender ship-like body (Thomas and Sclavounos, 2006) with fore-aft symmetry similar to a spheroid. In the reference, sway added masses are found with the 3D Rankine source method SWAN. In essence, the change in the hydrodynamic properties is attributable to the fact that in bounded flow the acceleration of water particles in the vicinity of the ship hull is aggrevated and also associated damping becomes more pronounced. The presence of the wall raises the question whether reflecting waves might affect the results even at low Froude numbers. The most and least narrow cases are expanded on for this investigation. Results for the side force and yaw moment coefficients are plotted in Figure 5 additionally. It is seen that the sway force coefficients are less sensitive to free surface effects than the yaw moment coefficients. While $Y_{\dot{v}}$ and Y_v hardly differ at all from the double-body results $N_{\dot{r}}$ and N_r exhibit a deviation by approximately 10%. It is assumed that this trend is attributable to the choice of the test parameters for the pure yaw case (ω'=4). In case of a vertical restriction the derivatives follow a similar trend when plotted against the ratio of water depth h to ship draft T. Here the boundedness of the flow also causes more fluid obstruction (Figure 5). The influence of heave and trim was not considered in the present investigation.

The Inland Waterway Vessel. Pure sway and yaw tests are now conducted for the inland waterway vessel (Table 2) in a narrow and shallow flow. The same time step and space discretization studies are performed. In what follows, given results are computed on a grid of $0.9{\cdot}10^6$ cells. The test parameters are ω'=2, y_A=1m for pure sway and ω'=4, ψ_A=2.3° for pure yaw. Figure 6 shows that the trends seen for the spheroid are also observed for the ship. Besides that the plots show all other derivatives needed to populate the maneuvering model (4). In absence of rudder action or any other controls, the inherent stability behaviour of the dynamic system can be studied by turning to the eigenvalues of the system matrix $\mathbf{A} = -\mathbf{M}^{-1}\mathbf{N}$ where $\mathbf{M}$ is the matrix acting on $\dot{\mathbf{x}} = [\dot{v}\ \dot{r}]^T$ and $\mathbf{N}$ the matrix acting on $\mathbf{x} = [v\ r]^T$ in

(4) because a solution to (4) with zero right hand side is

$$\mathbf{x}(t) = e^{\mathbf{A}t}\mathbf{x}_0 \tag{11}$$

It can be shown that the system matrices found for various restricted maneuvering environments all have one eigenvalue λ with positive real part $\Re(\lambda)$ giving way to unbounded amplification as a response to external excitation. In the considered environment, such an excitation can be suction forces generated by the presence of a canal wall or another ship. It is seen that the magnitude of the positive real part eigenvalues increases with decreasing water depth and distance to the wall (Figure 4). Mucha and el Moctar (2013) discussed the narrow water influence on the actual maneuvering trajectory for a large tanker and the related need for increased control action.

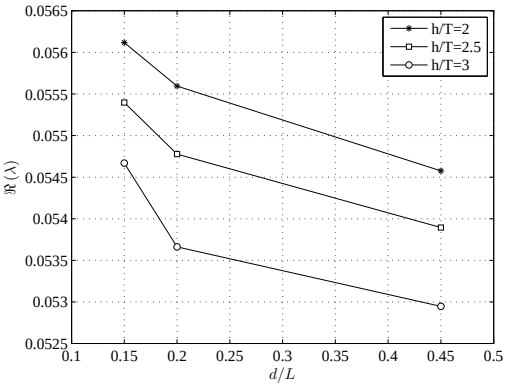

Figure 4: VESSEL: POSITIVE REAL PART EIGENVALUES AGAINST NONDIMENSIONAL WALL DISTANCE

5 CONCLUSIONS

PMM tests were replicated by a numerical method based on the solution of the RANS equations. For a spheroid it was shown that it is possible to find hydrodynamic sway and yaw acceleration derivatives with satisfactory accuracy. The influence of lateral and vertical flow restrictions was shown to significantly increase these quantities. For low Froude numbers, and moderate test frequencies, it was observed that through the presence of a wall there is no significant influence of the free surface on the hydrodynamic derivatives. Further investigations expanded on the derivation of a linear set of maneuvering coefficients for a typical inland waterway vessel for various restricted maneuvering environments. It was shown that the narrow and shallow water effect have a destablizing effect on the motion of the vessel in the horizontal plane. The computational effort for the host of virtual PMM tests was remarkably high and in absence of appropriate computational resources prohibitive. A more sophisticated validation and verification methodology *e.g.* through comparison with model tests is needed to gain more insight into the suitability of the presented method for maneuvering prediction in restricted waters.

6 ACKNOWLEDGMENTS

The Authors would like to thank the Federal Waterways Engineering and Research Institute (BAW) for use of computational resources and the financial support of this work.

7 REFERENCES

Cd adapco, 2013, *STARCCM+-User-Guide 8.04.007*

Ferziger, J., Peric, M., 1996, *Numerische Strömungsmechanik*, Springer

Liu, Z., Larsson, L., 2011, *CFD Prediction and Validation of Ship-Bank Interaction in a Canal*, Proceedings of the 2nd International Conference on Ship Manoeuvring in Shallow and Confined Water: Ship-to-Ship Interaction

Menter, F.R., 1994, *Two-Equation Eddy-Viscosity Turbulence Models for Engineering Applications*, AIAA Journal, Vol. 32, No. 8, pp. 1598-1605

Mucha, P., el Moctar, O., 2013: *Ship-Bank Interaction of a Large Tanker and Related Control Problems*, Proceedings of the 32nd International Conference on Ocean, Offshore and Arctic Engineering OMAE 2013

Newman, J.N., 1978, *Marine Hydrodynamics*, MIT Press

Renilson, M.R., 1986, *A Note on the Fluid Memory Effects and Non Linearities Involved in Oscillatory Ship Model Manoeuvring Experiments*, Proceedings of the 9th Australian Fluid Mechanics Conference

Söding, H., von Graefe, A., el Moctar, O. and Shigunov, V., 2012, *Rankine source method for seakeeping predictions*, Proceedings of the 31st International Conference on Ocean, Offshore and Arctic Engineering OMAE 2012

Stern, F., et al., 2011, *Experience from SIMMAN 2008: The First Workshop on Verification and Validation of Ship Maneuvering Simulation Methods*, Journal of Ship Research, Vol. 55, No. 2, pp. 135147

The International Towing Tank Conference - Recommended Procedures and Guidelines, 2005, *Testing and Extrapolation Methods Manoeuvrability Captive Model Test Procedures*, 7.5-02-06-02

Thomas, B. S., Sclavounos, P. D., 2006, *Optimal Control Theory Applied to Ship Maneuvering in Restricted Waters*, Readings in Marine Hydrodynamics, Volume Published in Honor of Professor J. Nicholas Newman

Tuck, E.O., 1978, *Hydrodynamic Problems of Ships in Restricted Waters*, Ann. Rev. Fluid Mechanics, No.10, pp. 33-46

Yoon, H., 2009, *Phase-averaged Stero-PIV Flow Field and Force/Moment/Motion Measurements for Surface Combatant in PMM Maneuvers*, Ph.D. thesis, The University of Iowa

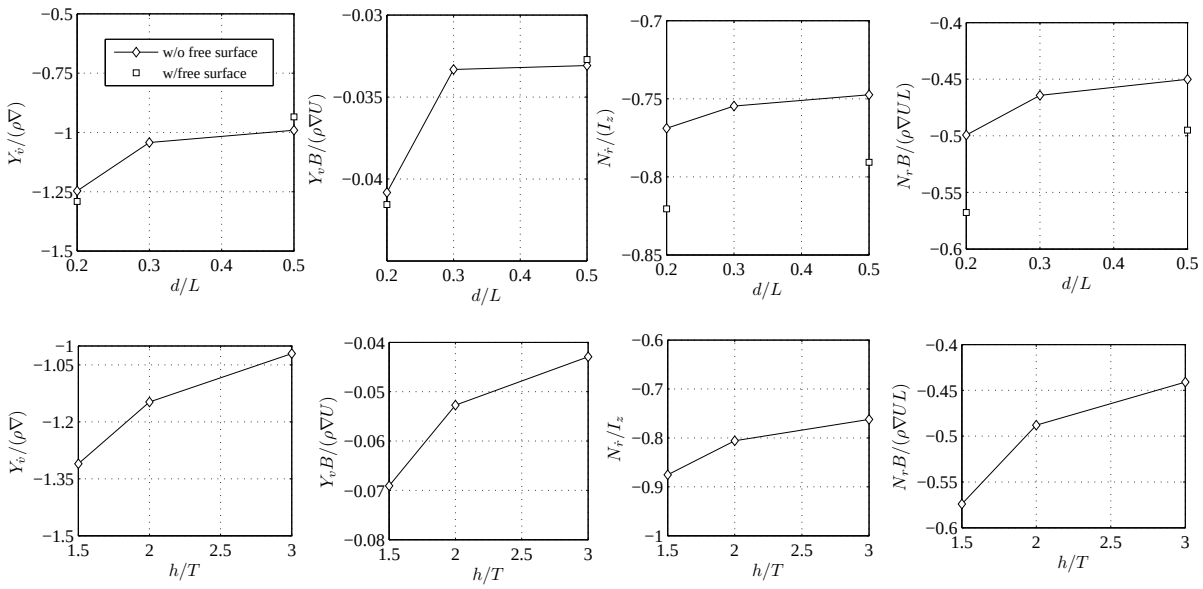

Figure 5: SPHEROID: SWAY FORCE AND YAW MOMENT DERIVATIVES AGAINST NONDIMENSIONAL WALL DISTANCE d/L AND WATER DEPTH-DRAFT RATIO h/T

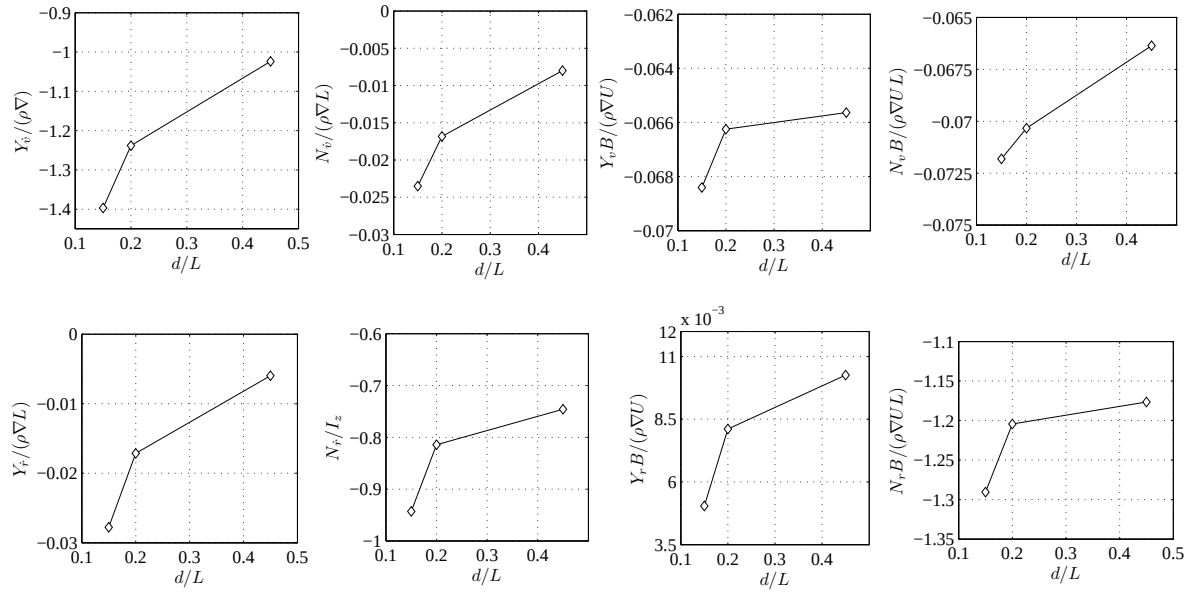

Figure 6: VESSEL: LINEAR HYDRODYNAMIC DERIVATIVES FOR SWAY AND YAW AGAINST NONDIMENSIONAL WALL DISTANCE d/L FOR h/T=2